

Computer Determination of $2V$ and Indicatrix Orientation from Extinction Data¹

F. DONALD BLOSS

Department of Geological Sciences

DEAN RIESS

Department of Mathematics

Virginia Polytechnic Institute and State University,
Blacksburg, Virginia 24061

Abstract

Using a detent spindle stage one can determine the optic axial angle, $2V$, to a fraction of a degree and, simultaneously, the spindle settings that correctly orient the crystal's indicatrix for measurement of refractive indices α , β , γ (or ϵ and ω). Experimental procedure involves setting the spindle stage so that the reading S on its protractor scale is successively 0° , 10° , 20° , . . . 180° . For each such setting S , the microscope stage is rotated until the crystal becomes extinct. The microscope stage readings M_s for which crystal extinction is observed—namely M_0 , M_{10} , M_{20} , . . . M_{180} —are analyzed by a least-squares computer technique which refines the coordinates for the two optic axes, calculates $2V$, and locates the three principal vibration axes with a potential accuracy not routinely available previously.

For an adularia from St. Gotthard, a set of 19 extinction measurements (M_0 , M_{10} , . . . M_{180}), here called trial (1), plus a second set of 18 extinction measurements (M_5 , M_{15} , . . . M_{175}), here called trial (2), observed at wavelengths 433 nm, 566 nm, and 666 nm yielded the following results:

λ (nm)	Trial	$2V_x$	X		Y		Z	
			S	E	S	E	S	E
433	(1)	63.66	87.57	86.56	172.96	143.19	0.13	126.60
	(2)	63.58	87.70	86.74	173.35	143.09	0.14	126.72
	Av.	63.62	87.64	86.65	173.15	143.14	0.13	126.66
566	(1)	64.92	87.27	86.28	172.37	142.70	0.08	127.05
	(2)	65.04	87.21	86.39	172.46	142.71	179.94	52.94
	Av.	64.98	87.24	86.33	172.42	142.70	0.01	127.06
666	(1)	65.18	86.69	86.11	171.49	143.14	179.58	53.42
	(2)	65.74	87.52	86.30	172.54	143.27	0.26	126.48
	Av.	65.46	87.10	86.20	172.02	143.20	179.92	53.47

where we define S as the spindle setting that would bring X , Y , or Z into the plane of the microscope stage, and E as the angle between X , Y , or Z and the spindle axis. Results for $2V_x$ clearly demonstrate dispersion of the optic axes ($r > v$). The relatively regular variation in the average S and E angles observed from 433 to 666 nm for X , the acute bisectrix, suggest it undergoes dispersion. The obtuse bisectrix, Z , appears not to, but Y possibly does. If so, the adularia must be optically monoclinic. However, the possibility remains that dispersion of Z is so small as to be undetectable.

Accuracy of the method decreases to the extent that the crystal happens to be oriented with a principal axis parallel to the spindle axis. Accuracy increases if a Nakamura plate or Macé de Lepinay half-shadow quartz wedge (or similar device) is used to refine extinction measurements.

The method applied here to adularia is applicable to studying anisotropic inclusions within transparent isotropic materials like glass or diamond. Although errors might be introduced to the extent that inclusion and host differ in refractive index, the resultant determinations of $2V$ and of dispersion of the optic axes help identify the inclusion without damage to the host.

¹ Computer programs written by David Upshaw under the direction of the authors.

Introduction

Using the detent spindle stage of Bloss and Light (1973) and the computer techniques developed by the writers from the equation of Joel (1966), one can now determine $2V$ and locate X , Y , and Z for a single crystal with potentially greater accuracy than has been heretofore possible. Because interference figures are not used, the observer requires little prior training in optical crystallography to collect the data. He needs only to rotate the crystal to extinction under the polarizing microscope for each spindle stage setting S (from 0° to 180° at 10° intervals). Thus minute crystals, if untwinned, can be handled with confidence.

By using light of different wavelengths while making accurate extinction measurements, an observer can determine whether a crystal is optically triclinic (X , Y , and Z all show dispersion), monoclinic (only two of the three show dispersion), or orthorhombic

(none of the three show dispersion). Exceptions to this arise if the dispersion of X , Y , or Z is too small to be detectable relative to experimental error.

Experimental Methods

Cement the crystal under study (or the transparent isotropic grain containing an anisotropic inclusion) to the tip of a needle or glass capillary tube with the glue-molasses mixture described by Wilcox (1959). After the cement is thoroughly dry, insert the needle with attached grain into the hypodermic tube that constitutes the spindle of the detent spindle stage. Next rotate the microscope stage until, as judged by eye, the spindle and needle are oriented E-W with the needle pointing west (Fig. 1). Record this reading as $\sim M_R$.

The visually estimated reading $\sim M_R$, can next be refined by an optical technique to determine M_R , the microscope stage reading which orients the spin-

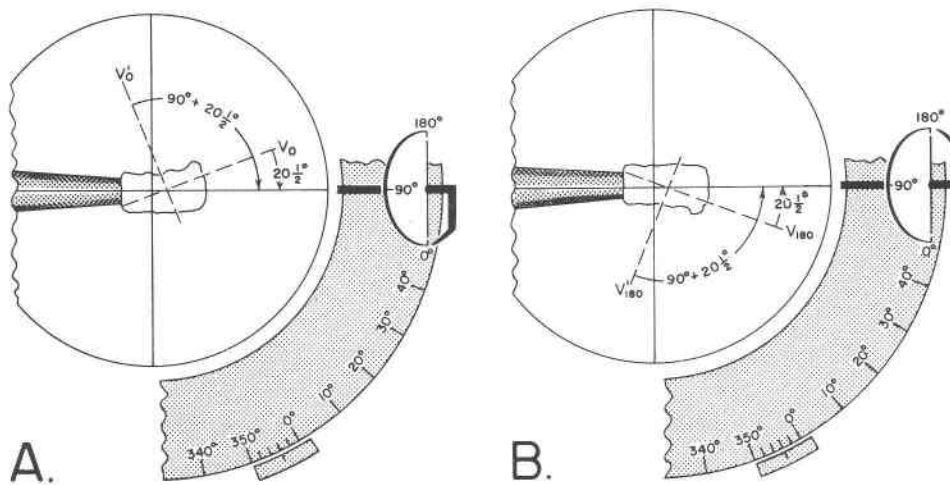


FIG. 1. (A) Sample field of view imposed on a schematic partial drawing of the microscope stage and spindle as seen after the spindle (set to read $S = 0^\circ$) has been visually aligned with the E-W crosshair, the spindle tip pointing west. (The reversal of images by the microscope makes the tip appear to point east within the field of view). A low-power objective, if used, will permit more of the spindle to be seen within the field of view during the alignment. As shown, M_E equals 356° for this example.

The dashed lines represent the crystal's mutually perpendicular vibration directions, v_0 and v'_0 . These lie in the plane of the microscope stage to the extent that (1) light is normally incident on the grain surfaces, and (2) the refractive index of the immersion oil surrounding the grain is close to the grain's refractive index for light vibrating parallel to v_0 or v'_0 . If the microscope stage were rotated clockwise until the crystal becomes extinct, v_0 would be E-W and the stage reading, symbolized M_0 , would be $16\frac{1}{2}^\circ$ for this example.

(B) Similar to (A) in that the microscope stage reading is again M_E . Now, however, the spindle is set to read 180° on its protractor stage so that the crystal is upside down from its position in (A). The privileged directions labelled v_{180} is actually that labelled v_0 in (A). If the microscope were rotated anticlockwise until the crystal becomes extinct, v_{180} would be E-W and the stage reading, symbolized M_{180a} , would be $339\frac{1}{2}^\circ$.

dle axis *exactly* E–W. Following Wilcox and Izett (1968, p. 270), we refer to M_R as the *reference azimuth*; note, however, that their reference azimuth orients the spindle axis N–S. To determine setting M_R :

- (1) Set the spindle to read 0° on its protractor scale, then rotate the microscope stage *clockwise* from position $\sim M_R$ until the crystal becomes extinct. Record this extinction position as M_0 .
- (2) Next set the spindle to read 180° and rotate the microscope stage *anticlockwise* from position M_0 until the crystal again becomes extinct. Record this extinction position as M_{180a} .

Operations (1) and (2) should each be performed at least five times so that M_0 and M_{180a} represent the average of at least five extinction readings. Although it will not be demonstrated here, M_R is necessarily the microscope stage reading midway between M_0 and M_{180a} . As a rule, therefore,

$$M_R = (M_0 + M_{180a})/2 \quad (1)$$

For example, if $M_0 = 194^\circ$ and $M_{180a} = 86^\circ$, then from Equation (1), $M_R = 140^\circ$. The value for M_R , however, will be 180° in error if readings M_0 and M_{180a} are on opposite sides of the 0° graduation of the microscope stage. To illustrate, if $M_0 = 24^\circ$ and $M_{180a} = 350^\circ$, Equation (1) yields an M_R of 187° whereas the true M_R equals 7° . Comparing the value of M_R obtained from Equation (1) with its visually estimated value $\sim M_R$ will always prevent such gross errors. Note that Equation (1) yields the correct value of M_R if we set M_{180a} equal to -10° rather than 350° . It is wise to be sure that M_R is very accurately known prior to each study because an error in M_R introduces a systematic error in the calculations of $2V$ and in locating the principal vibration axes. However, such systematic error can be reduced or eliminated (as will be discussed under "Results").

Let M_S represent the microscope stage reading that brings a crystal to extinction while the spindle stage reading is S . The crystal then has one vibration direction (v_s) oriented E–W and its second vibration direction (v_s') oriented N–S. We now define E_S to represent the angle between the spindle axis and a vibration direction v_s .² We already know M_R , the

microscope stage setting which orients the spindle axis precisely E–W. Thus, if we know M_S , the microscope stage reading that orients vibration direction v_s precisely E–W, then we can determine E_S because

$$E_S = M_S - M_R \quad (2)$$

As for all extinction angles, we restrict E_S to values in the range $0 \leq E_S \leq 180^\circ$. If Equation 2 yields an E_S value outside this range, add or subtract 180° from this value so as to bring it in range without changing its orientation in space. For example, suppose M_R equals 7° and M_{20} equals 262° . Equation (2) indicates that E_{20} equals 255° , so we subtract 180° to obtain $E_{20} = 75^\circ$.

Routine Procedure and Plotting

Having determined and set M_R very precisely, set the spindle to read 0° on its protractor—that is, $S = 0^\circ$ —then rotate the microscope stage clockwise until the crystal becomes extinct. Record this microscope stage reading and label it M_0 . Then change the spindle setting by 10° so that $S = 10^\circ$, and again rotate the microscope stage until the crystal becomes extinct; record this stage position and label it M_{10} . This process is repeated to determine the values for M_{20} , M_{30} , \dots , M_{180} as the spindle stage setting S is changed by 10° increments. The detent stage³ of Bloss and Light (1973) has a spindle that "clicks" into place at $S = 0^\circ, 10^\circ, \dots, 180^\circ$. This increases speed and accuracy for setting the spindle in determining $M_0, M_{10}, \dots, M_{180}$.

The coordinate system for plotting spindle stage data becomes apparent if we draw a crystal as if it were a huge sphere at the spindle's tip (Fig. 2). An optical direction can now be specified by stating its S and E_S coordinates— S being the setting of the spindle stage that orients this direction into the plane of the microscope stage, and $E_S (= M_S - M_R)$ being the angle between this direction and the spindle axis. In Figure 3, the stereonet is oriented so that its great circles represent some of the family of planes that are hinged on the spindle axis when this axis is E–W. To emphasize this, a spindle handle (set to read $S = 0^\circ$) is drawn relative to these great circles, which are labelled $S = 0^\circ, S = 10^\circ, \dots, S = 180^\circ$ because they represent planes through the crystal that become parallel to the plane of the microscope

² In effect, E_S represents the extinction angle for vibration direction v_s as measured relative to the spindle stage axis rather than relative to some crystallographic direction, for example, relative to the trace of a cleavage plane.

³ Available commercially from Technical Enterprises, Inc., P. O. Box 2604, Cambria Station, Christiansburg, Virginia 24073.

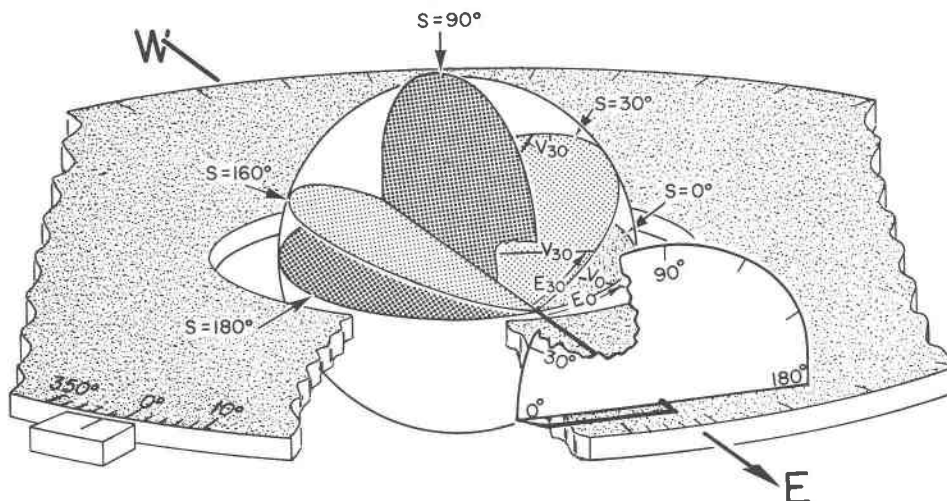


FIG. 2. Hypothetical crystal drawn as a huge sphere attached to the tip of the spindle. The planes hinged on the spindle axis represent a few of those planes through the crystal's indicatrix that can be brought parallel to the microscope stage by setting the spindle to read $S = 0^\circ$, 30° , 90° , 160° , 180° on its protractor scale. These planes are referred to as $S = 0^\circ$, $S = 30^\circ$, etc., according to the spindle setting necessary to bring them parallel to the microscope stage. The crystal's two privileged directions v and v' for light vibrating within these "S planes" are subscripted according to the particular S plane in which they lie. The microscope stage reading of 358° is presumed here to equal M_R , the reference azimuth or setting which orients the spindle axis precisely E-W.

To measure the extinction angle (E_S) for a given privileged direction relative to the spindle axis, for example E_{30} , set the spindle at $S = 30^\circ$ on its protractor scale so as to bring v_{30} and v'_{30} parallel to the microscope stage. Rotate the microscope stage clockwise until the crystal becomes extinct, say at a stage reading (M_{30}) of 25° . Whereas stage reading M_R sets the spindle axis E-W, stage reading E_{30} sets vibration direction v_{30} to be E-W. Thus

$$E_{30} = M_{30} - M_R = 25^\circ - (358^\circ)$$

If we consider 358° as a reading of -2° , then E_{30} equals 27° .

stage as the spindle is set at $S = 0^\circ$, 10° , \dots 180° . Any particular direction in a given S plane can be plotted stereographically by counting, along the comparable great circle S, a number of degrees equal to E_S for this particular direction. For example, suppose the settings $S = 20^\circ$ and $E_{20} = 75^\circ$ bring the crystal to extinction; the crystal vibration direction, v_{20} , which is horizontal and E-W in this extinction position, then plots as shown in Figure 3. The other vibration direction, v_{20}' , which is then horizontal and N-S, plots on the same great circle ($S = 20^\circ$) but at 90° from v_{20} ; thus E_{20}' equals 165° ($= 75^\circ + 90^\circ$) as shown. As is customary for all vibration directions, v_{20} and v_{20}' are plotted stereographically in the orientations they would have if the spindle were oriented E-W and if S were equal to 0° . If all vibrations, v_0 , v_0' , v_{10} , v_{10}' , \dots v_{180} , v_{180}' are plotted, the extinction curves for the crystal result (Fig. 4).

Computer Techniques

The measured values of M_R and of the eighteen (M_S) readings of the microscope stage which produce crystal extinction as S is set at 0° , 10° , \dots 170° constitute input into two computer programs⁴ that calculate $2V$ and the S, E_S coordinates of the two optic axes, of their acute and obtuse bisectrices, and of the optic normal (Fig. 5). From the input, the computer can not determine whether the acute

⁴The two computer programs used to analyze the present extinction data are now being compiled into a single program that will also calculate estimated standard deviations. For use in the interim, copies of these two programs can be secured by ordering NAPS Document Number 02204 from Microfiche Publications, 305 East 46th Street, New York, New York 10017; remitting in advance \$1.50 for microfiche or \$5.00 for photocopies. Please check the most recent issue of this journal for the current address and prices.

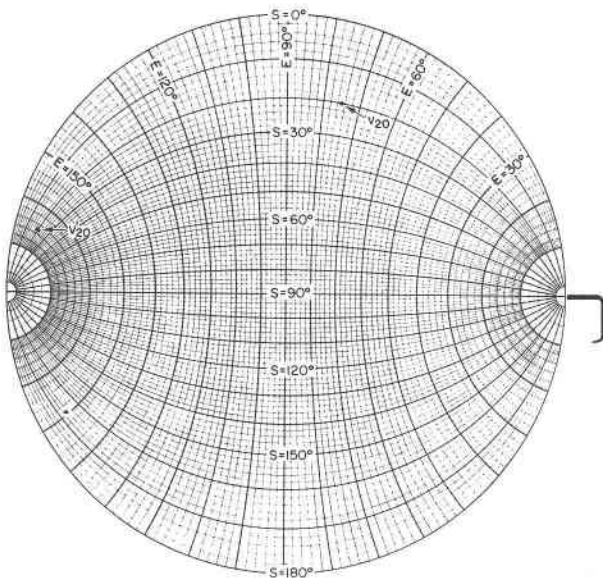


FIG. 3. Orientation of stereonet used for plotting a crystal's vibration directions if their S , E_s coordinates are known.

bisectrix represents X or Z . To ascertain this, the observer must use an accessory plate—that is, a quartz wedge or first-order-red plate—to determine whether one (and thus all) vibration(s) on the polar extinction curve corresponds to the slow or fast wave relative to one (and thus all) on the equatorial curve. For our adularia example, the polar curve proved to be the site of slow γ' vibrations. Consequently, the obtuse bisectrix—whose computer-determined coordinates S , E_s placed it on the polar curve—necessarily represented Z . This knowledge established the crystal's optic sign to be negative and permitted the directions, reported as 'acute bisectrix,' 'obtuse bisectrix,' and 'optic normal' in the computer print-out (Fig. 5) to be equated to X , Z and Y , respectively.

Results

A very small crystal of adularia was mounted on the spindle of a detent stage which, unlike the standard detent stage, had detents every 5° . Narrow-band-pass filters were used to isolate light of wavelengths 433, 566, and 666 nm which are fairly close to the G , D , and C Fraunhofer lines. For each wavelength, the crystal's extinction positions were determined by Dr. Michael W. Phillips as the spindle stage was rotated at 10° intervals. For each wavelength, two sets of extinction data were collected

(Table 1). For Set 1 the starting point was $S = 0^\circ$; for Set 2 it was at $S = 5^\circ$. The computer programs previously cited processed both sets, converting microscope stage extinction positions, M_s , into extinction angles E_s by use of Equation 2 (and the input M_R value), then calculating $2V$ and the S , E_s coordinates of principal vibration axes X , Y , and Z for each wavelength. As already discussed, the direction labelled 'obtuse bisectrix' in the program output was established to be Z (and the crystal to be optically negative) by use of an accessory plate. Results were as tabulated in the abstract. The average values for each wavelength reveal a small but definite dispersion ($r > v$) of the optic axes for this adularia, thus $2V_G = 63.8^\circ$, $2V_D = 65.1^\circ$, $2V_C = 65.7^\circ$. Systematic changes with wavelength of the S , E_s coordinates for X and possibly for Y indicate their dispersion. For Z , however, its S , E_s coordinates differ as little between wavelengths 433, 566, and 666 nm as they do between Sets 1 and 2 for an individual wavelength. Probably, therefore, Z undergoes no dispersion and the crystal is optically monoclinic. If several more sets of extinction data were collected at each wavelength—and if experimental

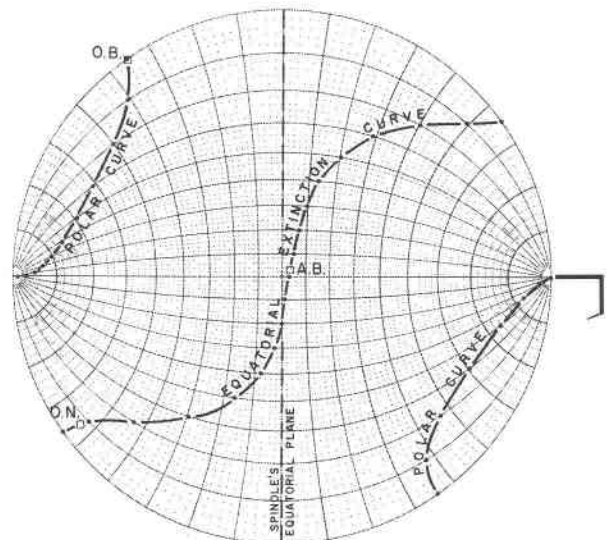


FIG. 4. Extinction curves for adularia for wavelength 433 nm as plotted from the extinction data in set 1, Table 4. See Figure 5 for the computer-determined locations of the acute bisectrix (AB), obtuse bisectrix (OB) and optic normal (ON) which have been added to these curves (small squares). Figure 5 also contains the E_s values (as determined by the computer from the M_s and M_R values) which were used in plotting these extinction curves. Note that E_s and $E_s + 90^\circ$ locates the two vibration directions that plot on a given great circle of the stereonet.

ADULARIA USING EVEN VALUES

WAVELENGTH = 433 MR 180.95

S= 0.0	MS=126.80	ES= 35.85
S= 10.00	MS=131.50	ES= 40.55
S= 20.00	MS=140.90	ES= 49.95
S= 30.00	MS=151.90	ES= 60.95
S= 40.00	MS=160.40	ES= 69.45
S= 50.00	MS=167.60	ES= 76.65
S= 60.00	MS=171.10	ES= 80.15
S= 70.00	MS=173.80	ES= 82.85
S= 80.00	MS=176.00	ES= 85.05
S= 90.00	MS=177.70	ES= 86.75
S=100.00	MS=179.90	ES= 88.95
S=110.00	MS=181.20	ES= 0.25
S=120.00	MS=183.70	ES= 2.75
S=130.00	MS=188.70	ES= 7.75
S=140.00	MS=197.40	ES= 16.45
S=150.00	MS=210.50	ES= 29.55
S=160.00	MS=224.10	ES= 43.15
S=170.00	MS=233.30	ES= 52.35
S=180.00	MS=235.10	ES= 54.15

OPTIC AXIAL ANGLE= 63.66

OPTIC AXIS A S= 61.56 ES= 105.27
 R= 0.848290 S= -0.263408 T= 0.459368
 OPTIC AXIS B S= 144.60 ES= 68.56
 U= 0.846311 V= 0.365499 W= -0.387516

LEAST SQUARES RESIDUAL= 0.0004031

VECTOR AB S= 87.57 ES= 86.56
 VECTOR OB S= 0.13 ES=126.60
 VECTOR ON S= 172.96 ES=143.19

FIG. 5. Typical computer output from Program 2. The S , M_S data which represent in-put are printed out so that punching errors in these cards can be more easily detected. The E_S values are calculated by the computer from each M_S value (and the M_R value).

error in measuring the extinction positions were reduced by use of a Nakamura plate, Macé de Lepinay quartz wedge, or similar device—a more definitive statement could perhaps be made with respect to the dispersion of X , Y , and Z in this adularia. However, the possibility will always remain that dispersion of a principal vibration axis is so weak that it is masked by even small experimental error.

The value of this technique now becomes apparent. The extinction angles observed with a sodium vapor light source or suitably filtered white light routinely yield accurate values for $2V_D$ and for the S , M_S values that will correctly orient the crystal so that the refractive indices α_D , β_D and γ_D can be compared to the index of the immersion oil. Using appropriate monochromatic wavelengths, the disper-

sion of the optic axes—for example, $2V_C$, $2V_D$, $2V_G$ —can be measured quantitatively. In addition, the dispersion of X , Y , and/or Z (or, less certainly, the lack thereof) can also be determined so that in some cases a biaxial crystal can be shown to be optically orthorhombic, monoclinic, or triclinic.

The coordinates (S , E_S) as computed for X , Y , and Z permit the crystal to be oriented so that its indices α , β , and γ can be measured free of errors from misorientation. The procedure is to set the microscope stage to read M_S —where M_S is obtained from the E_S and M_R values because from Equation (2), $M_S = E_S + M_R$. With M_S thus attained, vary the spindle stage setting until the crystal becomes extinct (whereupon the desired coordinate S is attained). For example, if $M_R = 180.6^\circ$ and if the coordinates for Z are $S = 0.1^\circ$ and $E_S = 126.7^\circ$, the microscope stage would be set at M_S equal to $307.3^\circ (= 126.7^\circ + 180.6^\circ)$ and the crystal would become extinct when S was set at (ca) 0.1° . For crystals of low or moderate birefringence, a 2 or 3° error in this setting produces negligible error in the index being measured. For microscopes with $N-S$ polarizers, the initial step would be to set the microscope stage to read $M_S + 90^\circ$.

It is wise to determine M_R with great care because, as mentioned earlier, any error in M_R produces a

TABLE 1. Microscope Stage Extinction Positions (M_S) for an Adularia from St. Gotthard*

S	M_S values, set one			S	M_S values, set two		
	433 nm	566 nm	666 nm		433 nm	566 nm	666 nm
0°	126.8°	127.8°	126.9°	5°	128.3°	129.0°	127.9°
10	131.5	131.7	131.3	15	135.5	135.5	134.9
20	140.9	140.7	140.8	25	146.8	146.6	145.2
30	151.9	151.7	151.7	35	156.2	156.4	155.0
40	160.4	160.1	160.2	45	164.7	163.7	163.6
50	167.6	166.8	167.2	55	169.8	169.7	168.7
60	171.1	171.5	170.6	65	172.5	172.4	172.8
70	173.8	173.6	173.7	75	176.3	175.1	174.1
80	176.0	175.7	176.0	85	176.6	176.8	175.8
90	177.7	177.2	176.5	95	179.0	177.5	178.3
100	179.9	178.8	179.0	105	180.5	180.0	180.0
110	181.2	180.7	180.9	115	182.3	182.0	182.6
120	183.7	183.3	184.6	125	186.1	185.9	187.3
130	188.7	189.1	188.1	135	191.6	192.8	192.4
140	197.4	197.3	197.2	145	203.8	204.5	204.2
150	210.5	211.5	213.7	155	216.9	218.5	219.6
160	224.1	224.7	226.3	165	229.7	230.1	229.8
170	233.3	233.3	232.2	175°	234.9	234.4°	235.2°
180°	235.1°	234.2°	235.0°				
M_R	180.95°	181.0°	180.95°	M_R	180.9°	181.0°	180.9°

* The microscope stage extinction positions (M_S) were determined by Dr. M.W. Phillips who kindly permitted use of this data. For each M_S reading, the computer calculates E_S —that is, $M_S - M_R$. For example, M_0 for $\lambda = 433$ nm equals 126.8° and thus $E_0 = 126.8 - 180.95 = -53.16^\circ$. The computer then adds 90° to obtain 36.85° , a value within the 0 to 180° range to which we conventionally constrain extinction angles (E_S).

systematic error in all values of E_S (cf Eq. 2). The program permits results to be computed not only for the empirically determined value of M_R but, at the same time, for values above and below it; we usually use values 0.1 and 0.2° above and below the measured M_R , but the spread can be as wide as one likes. As a rule, the least squares residual for the computations will minimize for empirical M_R or within 0.1° thereof. For example, extinction measurements for a synthetic nickel diopside crystal by Brenda Higgins (Table 2) yielded varying results depending upon the value assigned to M_R (Table 3). Note that the least squares residual was minimized for M_R values of 180.5 ($=$ empirical) and 180.6 . In a few instances where extinction measurements were made for three different wavelengths of light at each setting of S , the M_R values which minimized the least squares residuals sometimes differed (by 0.1°) from one wavelength to the other. To a certain extent, therefore, the additional degree of freedom introduced by varying M_R may in itself reduce the least squares residuals. The situation resembles the use of different temperature factors to decrease further the R values in crystal structure analyses.

This method of determining $2V$ and the orientation of the principal vibration axes probably exceeds all present methods in accuracy, particularly if the 18 extinction measurements were made with a Nakamura plate or Macé de Lepinay quartz wedge. Accuracy could perhaps be slightly increased by grinding the crystals into spheres or into cylinders co-axial with the spindle needle. This insures that the wave normal of the light would remain perpendicular to the microscope stage after entering the crystal. With an irregularly shaped crystal, this will not be true for certain settings S to the extent that (1) the refractive index of the oil differs from one or the other of the crystal's two indices and (2) the crystal surface on which light is incident is not parallel to the microscope stage.

Fortunately, there seems little need to grind the crystals into spheres or cylinders because errors due to irregular shape may be, to some extent, compensatory. Moreover, errors due to irregular shape could be decreased by making the measurements for two or more different mounts of the same crystal, then averaging the results. Primarily, to test the effect of irregular shape, a detent spindle stage study of a new mineral he was studying was made by Dr. M. G. Bown, who brought the crystal to extinction at maximum blackness. This same grain was then re-

TABLE 2. Spindle Stage Setting (S) and Microscope-Stage Extinction Positions (M_S) for a Nickel Diopside Crystal*

S	M_S	S	M_S	S	M_S	S	M_S
0°	217.6°	50	208.4	100	146.3	150	141.0
10	216.5	60	203.2	110	142.4	160	141.8
20	215.3	70	191.9	120	141.7	170	142.7
30	214.0	80	169.8	130	140.4	180°	143.3°
40	211.7	90	153.1	140	140.5		

* Each extinction position (M) represents an average of at least three measurements by Brenda Higgins for light of wavelength 533 nm.

moved and remounted in a different orientation on the spindle's needle and its extinctions measured (by F.D.B.) using a Macé de Lepinay quartz wedge. This latter technique yielded a smaller least squares residual and probably entailed less experimental error. The measured values of $2V$ compare as follows:

λ (nm)	500	600	666
(MGB)	44.6	47.3	45.2
(FDB)	45.8	45.5	45.0

TABLE 3. The Effect of Errors in M_R Values on Results of Computer Analysis of Data in Table 2*

	Test Values of M_R					
	180.0°	180.4°	180.5°	180.6°	180.7°	181.0°
Least squares residuals						
	0.0015	0.0005	0.0004	0.0004	0.0005	0.0011
Optic axial angle						
$2V$:	80.63°	79.91°	79.73°	79.56°	79.38°	78.86°
Optic axis A, coordinates						
S:	61.09°	67.11°	68.36°	69.53°	70.62°	73.51°
E:	172.05°	170.77°	170.44°	170.10°	169.77°	168.75°
Optic axis B, coordinates						
S:	167.11°	167.48°	167.57°	167.66°	167.74°	167.98°
E:	101.66°	101.61°	101.95°	102.01°	102.07°	102.25°
Acute bisectrix, coordinates						
S:	159.06°	158.05°	157.79°	157.54°	157.29°	156.54°
E:	141.44°	141.10°	141.01°	140.92°	140.83°	140.55°
Obtuse bisectrix, coordinates						
S:	174.55°	176.39°	176.84°	177.29°	177.74°	179.07°
E:	52.47°	52.55°	52.58°	52.61°	52.65°	52.76°
Optic normal, coordinates						
S:	78.68°	79.40°	79.58°	79.75°	79.92°	80.43°
E:	82.41°	80.97°	80.62°	80.26°	79.90°	78.83°

* Values of M_R which yielded the smallest least squares residuals and which are presumably the closest to correct are the empirically determined M_R value of 180.5° and a closely neighboring value of 180.6° .

Unfortunately, the crystal was lost while being remounted to use the Macé de Lepinay quartz wedge to compile another set of data.

Some orientations of a biaxial crystal on the spindle stage reduce the accuracy of this method. Unfavorable orientations result to the extent that a principal vibration axis approaches parallelism with the spindle axis. In such cases the equatorial extinction curve departs less and less from a great circle and this lack of distinctive characteristics prevents precise location of the two optic axes. Favorable orientations occur if an optic axis happens to be nearly perpendicular to the spindle axis. For the new mineral, the orientation studied by Dr. Bown was relatively unfavorable, but was changed to a favorable orientation prior to study by F.D.B.

Recently, Dr. Max Carman, while using a Macé de Lepinay quartz wedge and testing the technique in the senior author's laboratory, determined 2V at wavelength 500 nm to be 47.7° for one sanidine crystal and 48.0° for another from the same rock. The first crystal proved to be in a favorable orientation, one optic axis being at a 70° angle to the spindle axis, whereas the second was not, one optic axis being at an 8° angle to the spindle axis. Interestingly, a 0.1° change in the value of M_R , the reference azimuth, produced at most a 0.1° change in the computed value of 2V for the favorable orientation but a 0.6° change in 2V for the unfavorable orientation. The 2V values cited above were calculated using the empirical values for M_R .

Resume of Data Cards and Print-Out

Program 1; Sequence of Data Cards

TITLE (20A4). No restrictions. Prints at top of output. Include wavelength and observed M_R value.

KG (I2). Number of 4-card sets of S , M_S cards. Columns 1 and 2, right justified, no decimal point.

MR ('',F10.4). Value of M_R , in columns 2–11, with decimal point followed by not more than 2 places plus D0 (zero). Example: 180.95D0.

R,S,T,U,V,W, (6F8.4). Direction cosines of trial optic axis A (r,s,t) and B (u,v,w). Usually take 0.936, -0.219, 0.275; 0.319, -0.516, -0.795, each followed by D0 (zero), in columns 1–8, 9–16, 17–24; 25–32, 33–40, 41–48.

SS,MS (2F10.4). Spindle stage reading S [SS in program] in columns 1–10; associated M_S reading [MS] in program in 11–20. Punch 18 such cards, $S = 0^\circ$; $S = 10^\circ$, . . . $S = 170^\circ$ plus a duplicate

of each. D0 (zero) not required. If $KG = 8$, remove cards $S = 30, 80, 120$ and 170 from duplicate deck, then arrange the 32 remaining cards in order of S values to form 4-card sets as suggested here: $S = 0, 40, 90, 130$; $10, 50, 100, 140$; $20, 60, 110, 150$; $30, 70, 120, 160$; $40, 80, 130, 170$; $0, 50, 90, 140$; $10, 60, 100, 150$; $20, 70, 110, 160$.

IREP (I2). This is blank card if another title and more data are to follow (but contains 1 in column 2 if program is finished).

Program 1; Print-Out

For each 4-card set. (1) In-put values, S , M_S plus $E_S (=M_S - M_R)$. (2) Direction cosines of optic axes A and B which satisfy Eq. (3) relative to the 4-card set. These need not be in upper hemisphere. (3) S , E_S values of ends of optic axes A and B in the upper hemisphere.

After all 4-card sets. (1) Average values for direction cosines of A and B for all 4-card sets. (2) Their normalized values, and (3) the S and E_S values for the upper-hemisphere-ends of the optic axes thereby defined, and (4) the angle (obtuse or acute) between these ends. (5) The S and E_S coordinates for the acute bisectrix AB, obtuse bisectrix OB, and optic normal ON.

Program 2; Sequence of Data Cards

TITLE. No restrictions. Prints at top of output.

IN (I2). No. of S , M_S cards. Columns 1 and 2 only, right justified, no decimal.

IT0A (I2). Number of pairs of trial optic axes to be used. Columns 1 and 2 only, right justified, no decimal.

TSA, TMAP (2F10.4). S (Cols. 1–10) and E_S (11–20) for trial optic axis A . Decimal followed by up to 4 figures and ending with D0 (zero). Prepare another such card for optic axis B .

Further pairs of such cards, according to number of pairs (IT0A) of trial optic axes. Usually IT0A equals 1, because only one such pair of cards is needed. If Program 2 fails to converge, then it might be desirable to try several different pairs of trial optic axes.

SS, MS. A number (=IN) of S , M_S data cards. Use same cards as for Program 1 but no duplicates and arrange in order of S values: $0^\circ, 10^\circ, \dots, 170^\circ$.

KMR (I2). Number of M_R values to be used. Columns 1 and 2 only, right justified, no decimal.

MR ('',F10.4). Values of M_R one per card, up to KMR such cards. Columns 2–11, decimal fol-

lowed by up to four figures ending with D0 (zero).

IREP (I2). Blank card if another title and more data follow. Otherwise a 1 in column 2 if program is finished.

Program 2; Print-Out

Title, then M_R value, then S , M_S (and computed E_S) for input cards (SS, MS), then input coordinates (S , E_S) for trial optic axes and subsequent pairs until a solution is found. If no solution is found for any pair, program writes CHECK TRIAL OPTIC AXES FOR ERROR—but also check correct punching of MR and SS, MS cards. For a solution, the program prints: (1) Optic axial angle; (2) S , E_S coordinates and direction cosines for optic axes A and B ; (3) The least squares residual to seven decimal places. This is a measure of the success of the refinement and of the precision of the extinction measurements. (5) S , E_S coordinates for acute bisectrix AB, obtuse bisectrix OB, and optic normal ON.

Acknowledgments

We are grateful to Dr. Michael W. Phillips and to Brenda Higgins for placing their experimental data at our disposal. Our colleague, Professor Paul H. Ribbe, kindly read the manuscript at an early stage and made several helpful suggestions. Dr. Michael G. Bown of the University of Cambridge was of great help during his stimulating sojourn in Blacksburg. The paper benefitted greatly from its careful review by Dr. Ray E. Wilcox of the U. S. Geological Survey, whose early recognition of the potential of the spindle stage places us all in his debt. The senior author is most appreciative for the support of much of this work by National Science Foundation Grant GA-32444.

Appendix: Mathematical Discussion

The equations used by Joel (1966) to find the optic axes vectors, \mathbf{a}_1 and \mathbf{a}_2 , are

$$(\mathbf{q} \cdot \mathbf{a}_1)(\mathbf{q} \cdot \mathbf{a}_2) - (\mathbf{q}' \cdot \mathbf{a}_1)(\mathbf{q}' \cdot \mathbf{a}_2) = 0 \quad (3)$$

where \mathbf{q}' is a direction within the indicatrix that is parallel to the spindle axis and \mathbf{q} represents a second direction—the so-called equivibration point—for which the crystal would exhibit the same refractive index as for light vibrating parallel to \mathbf{q}' . The solutions involve the determination of six unknowns, namely the three coordinates of \mathbf{a}_1 and the three coordinates of \mathbf{a}_2 in a rectangular xyz coordinate system. In all measurements, \mathbf{q}' is fixed and is taken to be the unit vector along the y axis, $(0, 1, 0)$. Since we have six unknowns, we need six equations to solve for \mathbf{a}_1 and \mathbf{a}_2 . Two of these equations come from forcing \mathbf{a}_1 and \mathbf{a}_2 to be unit vectors, *i.e.*, if we denote $\mathbf{a}_1 = (r, s, t)$ and $\mathbf{a}_2 = (u, v, w)$, then $r^2 + s^2 + t^2 = 1$ and $u^2 + v^2 + w^2 = 1$. Thus if there were absolutely no experimental error in determining each \mathbf{q} , one could perform experiments for only four different values of \mathbf{q} and then solve the resulting six equations to obtain \mathbf{a}_1 and \mathbf{a}_2 precisely.

The first program does exactly this, using Newton's Method (Bartle, 1967, p. 231) for six variables. Let the different values for \mathbf{q} (usually 19 in number—one for each 10 degree increment of S from 0° to 180°) be denoted by \mathbf{q}_k , $0 \leq k \leq 18$. Each \mathbf{q}_k is transformed into rectangular coordinates, where its x , y , and z coordinates are, respectively, $\sin 2E_s \sin S$, $\cos 2E_s$, and $\sin 2E_s \cos S$. For each \mathbf{q}_k , let

$$\begin{aligned} f_k(\mathbf{a}_1, \mathbf{a}_2) &= (\mathbf{q}_k \cdot \mathbf{a}_1)(\mathbf{q}_k \cdot \mathbf{a}_2) - (\mathbf{q}' \cdot \mathbf{a}_1)(\mathbf{q}' \cdot \mathbf{a}_2) \\ &= (\mathbf{q}_k \cdot \mathbf{a}_1)(\mathbf{q}_k \cdot \mathbf{a}_2) - sv \end{aligned} \quad (4)$$

Let

$$\hat{\mathbf{f}}(\mathbf{a}_1, \mathbf{a}_2) = \begin{pmatrix} f_{k_1}(\mathbf{a}_1, \mathbf{a}_2) \\ f_{k_2}(\mathbf{a}_1, \mathbf{a}_2) \\ f_{k_3}(\mathbf{a}_1, \mathbf{a}_2) \\ f_{k_4}(\mathbf{a}_1, \mathbf{a}_2) \\ r^2 + s^2 + t^2 - 1 \\ u^2 + v^2 + w^2 - 1 \end{pmatrix}, \quad (5)$$

where k_1, k_2, k_3, k_4 represent any four functions of Equation (4). The objective, of course, is to find vectors \mathbf{a}_1 and \mathbf{a}_2 so that all six components of $\hat{\mathbf{f}}(\mathbf{a}_1, \mathbf{a}_2)$ are zero. If this is so, then Equation (3) is satisfied for these four values of \mathbf{q}_k . Let $x_0 = (r_0, s_0, t_0, u_0, v_0, w_0)$ where (r_0, s_0, t_0) and (u_0, v_0, w_0) are initial guesses for \mathbf{a}_1 and \mathbf{a}_2 , respectively. (In all of our computations we used $(r_0, s_0, t_0) = (0.936, -0.219, 0.275)$ and $(u_0, v_0, w_0) = (0.319, -0.516, -0.795)$. These initial guesses need not be at all accurate. The above values worked in all of our computations no matter which material was being examined. Different initial guesses can be used as long as they are unit vectors and r_0 and u_0 are not negative.)

Our problem can be simply stated as: Find \mathbf{a}_1 and \mathbf{a}_2 such that $\hat{\mathbf{f}}(\mathbf{a}_1, \mathbf{a}_2) = 0$, the zero vector. Newton's Method to find a root, X^* , of a function of one variable, $h(X)$ —*i.e.*, find X^* such that $h(X^*) = 0$ —is as follows:

Let X_0 be an initial guess for X^* , and generate a sequence of points, $\{X_j\}$, $j = 1, 2, \dots$ by the formula:

$$X_{j+1} = X_j - f(X_j)/f'(X_j) \quad (6)$$

Stop the iteration when $|f(X_j)| < \epsilon$, where ϵ is sufficiently small enough to consider $f(X_j)$ essentially equal to zero.

Newton's Method for several variables (six, in our case) is of the same form, except that the derivative of the vector-valued function, $\hat{\mathbf{f}}(\hat{X})$ is the so-called "Jacobian" matrix, $J(\hat{X})$ (see Bartle, p. 231), where \hat{X} is a variable vector with six components. In our case the Jacobian is 6×6 and non-singular. Let $J^{-1}(\hat{X})$ denote the inverse of the Jacobian, and let the sequence of vectors $\hat{X}_j = (r_j, s_j, t_j, u_j, v_j, w_j)$ be generated by the formula:

$$\hat{X}_{j+1} = \hat{X}_j - J^{-1}(\hat{X}_j)f(\hat{X}_j), \quad (7)$$

where \hat{X}_0 is again the initial guess mentioned above. To avoid computing $J^{-1}(\hat{X}_j)$ for each j , Equation 6 can be solved for \hat{X}_{j+1} by using the IBM SIMQ subroutine on the equivalent equation,

$$J(\hat{X}_j)\hat{X}_{j+1} = J(\hat{X}_j)\hat{X}_j - \hat{\mathbf{f}}(\hat{X}_j), \quad (8)$$

which is merely a linear system of six equations in six unknowns. Stop this iteration at a value of j when all six components of $\hat{f}(\hat{X}_j)$ are less than some prescribed value ϵ . (We used fifty iterations, *i.e.*, the last value of j was fifty, and always obtained $\epsilon < 10^{-15}$). The first three components of this \hat{X}_j are used for \mathbf{a}_1 and the last three are used for \mathbf{a}_2 .

If there were no experimental errors in determining the q_k values, we would be finished at this point, because each measured q_k value would satisfy Equation (3) within 10^{-15} for the computed values of \mathbf{a}_1 and \mathbf{a}_2 . Because of the experimental error in q_k , however, this is not the case. Thus this procedure is repeated with a different set of four measured values of q_k . (Our program is written to perform this repetition eight times, although more can be used if certain values of q_k are suspected to be bad.) Lastly, the values computed for \mathbf{a}_1 and \mathbf{a}_2 in each repetition are averaged. These averages are normalized, *i.e.*, divided by their lengths to make them unit vectors, and this result is used for an initial approximation for \mathbf{a}_1 and \mathbf{a}_2 in the second program.

The values for \mathbf{a}_1 and \mathbf{a}_2 computed above do not exactly satisfy Equation (3) for each q_k due to its experimental error. Thus, we form the "residual least squares function"

$$F(\mathbf{a}_1, \mathbf{a}_2) = f_0(\mathbf{a}_1, \mathbf{a}_2)^2 + f_1(\mathbf{a}_1, \mathbf{a}_2)^2 + \cdots + f_n(\mathbf{a}_1, \mathbf{a}_2)^2, \quad (9)$$

where n is the number of experimental measurements (usually 19). An accelerated gradient method (Goldstein, 1967, p. 37) is used to find values for \mathbf{a}_1 and \mathbf{a}_2 which minimize $F(\mathbf{a}_1, \mathbf{a}_2)$.

To minimize a real-valued function of one variable, $g(X)$, we find the root, X^* , of its derivative, *i.e.*, $g'(X^*) = 0$. The process is theoretically the same here, except that $F(\mathbf{a}_1, \mathbf{a}_2)$ is a real-valued function of six variables and thus its derivative (see Bartle, 1967, p. 247) is its so-called "gradient," $\nabla F(\mathbf{a}_1, \mathbf{a}_2)$. This gradient is a vector-valued function with six components. Thus, finding \mathbf{a}_1 and \mathbf{a}_2 to make all six of the components of the gradient equal to zero is the same kind of problem as was solved by Newton's Method in the first program. This time, however, the initial approximation must be "close" to the true solution (Again, see Goldstein, 1967, p. 37), and thus X_0 is chosen as generated by the first program.

We have learned through computational experience that finding the optic axes is a very ill-conditioned problem, *i.e.*, small experimental errors for unfavorable crystal orientations can propagate large errors in \mathbf{a}_1 and \mathbf{a}_2 . In most of our computations, the residual least squares function, Equation (9), has a minimum value of the order 10^{-3} . If one or more measured value of q_k is bad, the \mathbf{a}_1 and \mathbf{a}_2 computed by the first program can vary widely with each set of four q_k values and their average may be sufficiently in error to prevent the second program from converging. We emphasize that this is due entirely to experimental error in q_k resultant from either operator error (including misadjustment of the microscope) or crystal inhomogeneity, since the mathematical theory underlying the methods is completely sound. The two programs combined will yield the best possible values for \mathbf{a}_1 and \mathbf{a}_2 within the limits of the experimental errors. Thus we stress the thorough examination of the values of \mathbf{a}_1 and \mathbf{a}_2 generated by the first program to eliminate those values of q_k which appear to be experimentally bad. If one or more of these bad values cannot be corrected and must be eliminated, the second program is easily modified by setting the variable IN in our program equal to the number of q_k values used.

References

- BARTLE, R. G. (1967) *The Elements of Real Analysis*. John Wiley and Sons, New York, 447 pp.
- BLOSS, F. D., AND J. F. LIGHT (1973) The detent spindle stage. *Amer. J. Sci., Cooper volume*, pp. 536-538.
- GOLDSTEIN, A. A. (1967) *Constructive Real Analysis*. Harper and Row, New York, 178 pp.
- JOEL, N. (1966) Determination of the optic axes and 2V: Electronic computation from extinction data. *Mineral. Mag.* **35**, 412-417.
- WILCOX, RAY E. (1959) Use of spindle stage for determining refractive indices of crystal fragments. *Amer. Mineral.* **44**, 1272-1293.
- , AND G. A. IZETT (1968) Optic angle determined conoscopically on the spindle stage. I. Micrometer ocular method. *Amer. Mineral.* **53**, 269-277.

Manuscript received, February 22, 1973; accepted for publication, July 13, 1973.